

## BUBBFIL ELECTROSPINNING OF PA66/Cu NANOFIBERS

by

**Ya LI<sup>a</sup>, Yuqin WAN<sup>b</sup>, Yan ZHANG<sup>a,c</sup>, Ji-Huan HE<sup>a,c\*</sup>, and Ping WANG<sup>a,c\*</sup>**

<sup>a</sup>National Engineering Laboratory for Modern Silk, College of Textile and Clothing Engineering, Soochow University, Suzhou, China

<sup>b</sup>Key Laboratory of Science and Technology of Eco-Textiles, Ministry of Education, Jiangnan University, Wuxi, China

<sup>c</sup>Jiangsu Wanggong Technology Co. Ltd., Suzhou, China

Original scientific paper  
DOI: 10.2298/TSC1603993L

*Different PA66/Cu nanofibers were prepared under various electrospinning parameters through bubbfil electrospinning. The process parameters were determined. Cuprum particles with different size were added to PA66 solution to produce PA66/Cu composite nanofibers. The influence of cuprum nanoparticle size on the PA66 nanofibers was analyzed.*

**Key words:** *bubbfil electrospinning, PA66/Cu nanofibers, particle size, influence, energy*

### Introduction

Due to the depletion of fuels and the increasing demand of energy for economic development, it is urgent to develop renewable energy technologies to sustain the economic growth. The 1-D nanostructured materials such as nanofibers (NF), nanowires [1], nanotubes [2], and nanorods [3] have attracted extensive attention due to their unique physical and chemical characteristics. In recent years, new functional composite NF have become the focus of studies for their unique properties compared to other nanostructured materials for applications in energy field. Until now, several methods such as template-assisted synthesis, chemical vapor deposition, self-assembly, wet chemical synthesis, and electrospinning have been applied to prepare nanofibrous materials [4]. Amongst these methods, electrospinning has been recognized as one of the most favorite technique.

Based on the mechanism of spider spinning and the principle of bubble dynamics, bubbfil electrospinning, also known as bubbfil electrospinning, has been proposed for large-scale production of NF materials. In order to lower the surface tension, bubbfil electrospinning uses polymers' or melts' bubbles or membranes to generate multiple jets for high efficient mass production of NF [5]. The jet ejection velocity in bubbfil electrospinning process can be as high as 100 m/s, thus a jet can reach the collector in just 0.001 second. The minimal diameter of the obtained fibers can be as fine as 5 nm. Therefore, bubbfil electrospinning is a facile method for fabrication of NF with high surface area to volume ratio and high porosity. An important attribute of the bubble is that it does not have any special requirement for the solution. The surface tension reduction only relates to the radius of the bubble and the inside and outside pressure ( $P_0$  and

\* Corresponding author; e-mail: hejihuan@suda.edu.cn, pingwang@suda.edu.cn

$P_1$ ) of the bubble, respectively, as expressed in  $T = 0.5r(P_1 - P_0)$  [6]. As long as the bubbles are small enough to allow the electrostatic force to break the surface tension of the bubble, jets will be generated and NF can be obtained. The diameter of the NF acquired depends largely on the bubble size. Meanwhile, the size of the bubbles can be adjusted through the inlet pressure, solution temperature, and the location of the top of the air tube [7].

Cuprum nanoparticles connected by or encapsulated in some precision components were often used in small devices to realize the function of electromagnetic shielding. Li *et al.* [8] produced Cu nanoparticles by reduction reaction in the water, then mixed in polyvinyl alcohol to generate PVA/Cu NF. Tao *et al.* [9] got silver/PA6 NF by electrospinning for preparation of Cu NF through reduction reaction.

Using bubbfil electrospinning, this paper conducted a study on mass-production of 1-D PA66/Cu NF to explore the potential of Cu-based nanofibrous materials for renewable energy applications such as solar cells, fuel cells, nanogenerators, hydrogen energy harvesting, and storage, lithium-ion batteries.

## Experimental

**Materials.** Nylon-66, with an average molecular weight of 15,000 g/mol purchased from Sigma Aldrich, anhydrous formic acid (88 wt.%) purchased from Sinopharm Chemical Reagent Co., Ltd., and copper sulfate (249.58, Shanghai Xin reagent factory) were used in these experiments, 40% joint-test formaldehyde solution and oleic acid were both purchased from Shanghai chemical reagent Co., Ltd., pure ethanol was from drug group Chemical Reagent Co., Ltd, sodium hydroxide (96% or higher) was purchased from reagent factory in Shanghai, polyvinylpyrrolidone with an average molecular weight of 50,000 g/mol was from national medicine group Chemical Reagent Co., Ltd. All materials used were without further purification.

**Solution preparation.** 22.68 g Cu sulfate and 33.3 mL formaldehyde were dissolved in 180 mL direct injection (DI) water. Pure ethanol and sodium hydroxide were dissolved in another 180 mL DI water. Oleic acid was added into different concentration of polyvinylpyrrolidone which was scattered in aqueous solution as the passivator in three flasks, and then the flasks were heated to 60 °C under nitrogen gas. These two solutions were prepared in the three flasks to prepare three different sizes of Cu nanoparticles. For preparation of Cu nanoparticle electrospinning solution, 1.5 g PA66 was dissolved into 7.5 g anhydrous formic acid, afterwards 0.2 g Cu particles were added into at the room temperature. The mixture was stirred at 80 °C until a homogeneous and transparent solution was obtained. The solution was then cooled down to room temperature for experiment.

**Electrospinning set-up.** Figure 1 shows the schematic of a bubbfil electrospinning set-up, which includes a high voltage generator, an air pump, a solution reservoir, a motor and a grounded collector.

Different voltage, such as 10 kv, 15 kv, and 20 kv, was applied to investigate the influence of voltage on the NF. The tip-to-collector distances in the experiment were also altered from 10 cm, 15 cm to 20 cm. Polymer solution was added into the solution reservoir which is connected to a gas pump through a hollow metal electrode. The positive voltage was applied to the electrode with a high voltage power generator (CPS-40K03VIT, Chungpa EMT Co., Korea). All electro-spin-

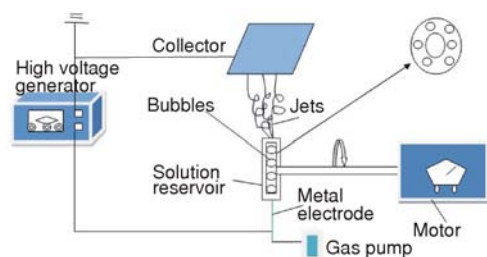


Figure 1. Device for bubbfil electrospinning

ning experiments were carried out at ambient conditions. The samples were placed in a vacuum oven for 24 hours at room temperature to remove the solvent residuals.

After the optimal process parameters were determined, Nylon66 NF with Cu nanoparticles in the range of 10-100 nm, 100-500 nm, and 500-1000 nm were prepared and calcinated at 800 °C using a muffle furnace.

Test and characterization of electrospun fiber meshes: Tensile test was conducted with a universal material testing machine (INSTRON 3365). The morphology of the electrospun NF was observed with a scanning electron microscope (SEM, Hitachi S4800, Japan) with an accelerating voltage of 3 kV and the captured images were analyzed with Image-Pro-Plus tool software to calculate the average diameter of the NF. X-ray photoelectron spectroscopy was used to analyze the existence of Cu element.

## Results and discussion

### Material fabrication

Figure 2 showed typical FE-SEM micrographs of the nylon6/66 NF webs. The average diameter of the obtained electrospun nylon6/66 fibers ranged from 80 nm to 200 nm, as

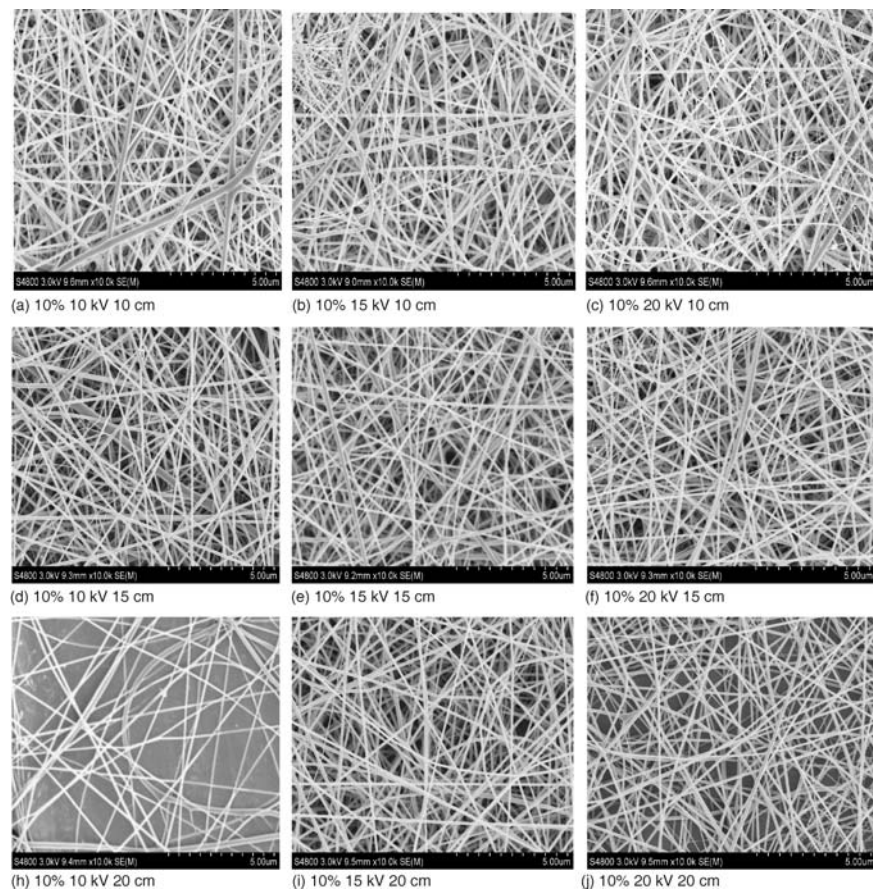


Figure 2. The FE-SEM micrograph of fibers bubble-electrospun from nylon6/66 dissolved in the formic acid 88 wt.% solutions at different parameters

shown in tab. 1. It can be seen that the surface of the fibers are mostly smooth and the NF produced at 20 kV voltage and 15 cm collecting distance are the finest and have the best uniformity.

**Table 1. The average diameters at the different parameters**

Parameter	a	b	c	d	e	f	h	i	j
Average diameter ( 5 nm)	114.29	118.98	107.76	115.26	103.43	97.55	123.79	105.83	101.22

For PA66 NF with 10~100 nm Cu nanoparticles incorporated, as shown in fig. 3(a), the average diameter was 287.54 nm. The Cu nanoparticles can barely be observed on the surface of the nanofibers indicating most of the Cu particles were embedded in the composite NF.

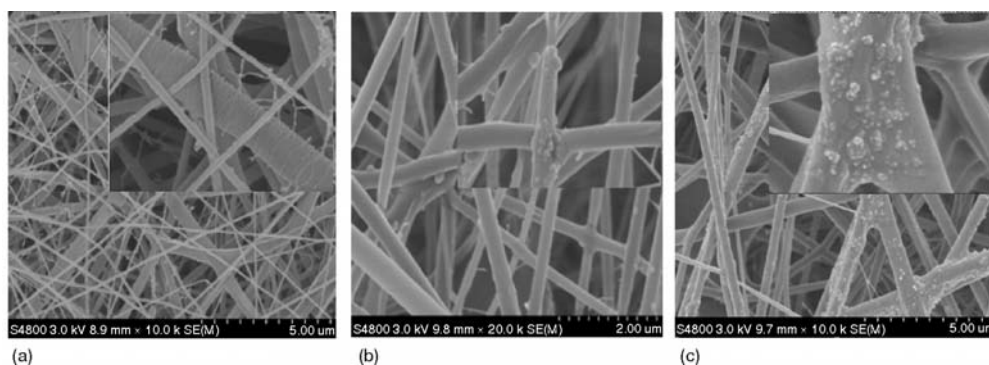


**Figure 3. Surface morphology of PA66/Cu composite NF membranes and adhesion in different particle sizes; (a) 10~100 nm, (b) 100~500 nm, (c) 500~1000 nm**

When the Cu nanoparticles size increased from 100 nm to 500 nm, the average diameter of PA66/Cu NF increased to 304.59 nm. More Cu nanoparticles were found on the fiber surface, as shown in fig. 3(b).

Regarding the 500~1000 nm Cu nanoparticles, the average diameter of the resultant PA66/Cu composite NF was 347.89 nm with diameter distribution ranging from 210~616.83 nm. Because of the Cu particle size is much larger than that of the composite NF, most Cu nanoparticles were found either in between the fibers or exposed on the surface of the fibers, as shown in fig. 3(c).

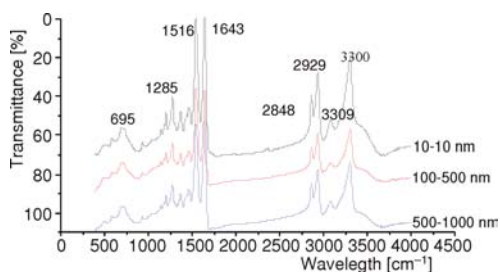


**Figure 4. The FTIR of PA66/ Cu composite NF membranes in different particle sizes**

#### Analysis of the FTIR

In order to examine whether Cu particles have influence on PA6/66, infra-red spectra of the three PA6/66-Cu NF were characterized by Fourier transform infrared (FTIR) spectroscopy (Nicolet 5700). The results were shown in fig. 4. The characteristic absorption bands at 1516  $\text{cm}^{-1}$  for C = O and 1643  $\text{cm}^{-1}$  for N-H in the three curves are consistent with the trans conformation absorptions of nylon-6/66. The (C-H)<sub>n</sub> ( $n > 4$ ) in the nylon6/66 exhibited stretching vibration band at the 695  $\text{cm}^{-1}$  and 1377  $\text{cm}^{-1}$  [10]. The



characteristic absorption bands at  $3300\text{ cm}^{-1}$  were due to the stretching vibration of O-H in the water. The characteristic absorption bands at  $3309\text{ cm}^{-1}$  were the vibration of the C ring within monomer form. The  $\text{CH}_3$  in nylon6/66 exhibited asymmetric and symmetrical vibration absorption peak at the  $2929\text{ cm}^{-1}$  and  $2848\text{ cm}^{-1}$ . It is clear that the addition of Cu had no effect on the chemical structure of nylon6/66 NF.

Due to the incorporation of different Cu nanoparticles in the NF, the strength of the NF membranes was different, as shown in tab. 2. The composite NF with Cu nanoparticles in the range of 10~100 nm showed the highest strength since most of the nanoparticles were embedded in the NF and hence the NF were reinforced by the particles. As the particle sizes increased, Cu nanoparticles were too big to be embedded in the NF. The incorporated Cu nanoparticles became the structure defects of those composite NF, therefore the fibers were weaker.

**Table 2. Mechanical properties of PA66/Cu composite nanometer fiber membranes with different sizes of nanoparticles**

Nanoparticle [nm]	Fracture strength [MPa]	Elongation at break [%]
10 nm~100 nm	4.65	10%
100 nm~500 nm	1.73	14%
500 nm~1000 nm	0.9	5%

*The XPS analysis of Cu/PA66 NF after calcination*

Figure 5 shows the X-ray photoelectron spectroscopy (XPS) spectra of sintered PA66/Cu composite NF studied by means of XPS-peak-differentiation-imitation analysis. Curve fitting of the spectra was done by a mixture of Gaussian and Lorentzian (GL) functions on a Shirley-type background. The parameter of % Gaussian-Lorentzian was set as 80%. When the particle sizes were between about 10~500 nm as shown in fig. 5(a), there were five resolved peaks, among which the peak of  $\text{Cu}_2\text{O}$  was at 932.9 eV, CuO peak existed at the position of 935.4 eV as a result of oxidation or chemical reaction with NaOH in the solution potentially. The rest peaks all ascribe to Cu, suggesting the mass proportion of Cu was about 82%. When the particle sizes were larger than 100 nm and smaller than 500 nm in fig. 5(b), the ingredients were shown completely Cu. For Cu between 500~1000 nm, five peaks were also could be seen in fig. 5(c), indicating CuO was produced at 933.9 eV. The main constituent part was Cu with the proportion of nearly 85%.

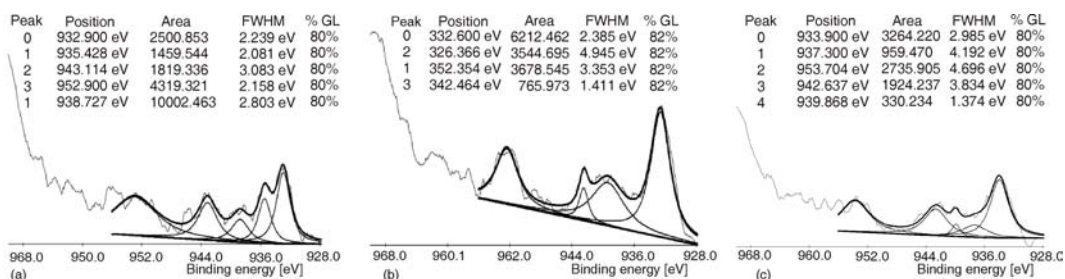


**Figure 5. The XPS spectra of Cu NF got after polymer burned in different particle sizes; (a) 10~100 nm, (b) 100~500 nm, (c) 500~1000 nm**

## Conclusions

The PA66 NF were fabricated through bubble-electrospinning process. The optimized process parameters were determined to be 10%, 20 kv, and 15 cm. Different PA66/Cu composite NF were prepared by adding different Cu nanoparticles to the electrospinning solution. The Cu particle size was found had significant influence on the mechanical properties of the composite NF. If too large Cu were incorporated, the structure of the composite NF would deteriorate and the NF became weaker. The FTIR analysis revealed that the addition of Cu had no effect on the chemical structure of PA6/66. The XPS analysis revealed that after sintering the main existence form of Cu element in PA66/Cu NF was Cu substance. This study proved that bubbfil electrospinning is an efficient and low cost technology for mass-production of functional composite NF that will be extremely useful in the near future for commercialization of nanocomposite fibers.

## Acknowledgment

The work is supported by PAPD (A Project Funded by the Priority Academic Program Development of Jiangsu Higher Education Institutions), "Six Talent Peak" of Jiangsu Province (ZBZZ-035), Doctoral Horizon Awards of Outstanding Talent Training Plan of Soochow University, National Natural Science Foundation of China (Grant No. 11402155), Natural Science Foundation of Jiangsu Province (Grant No. BK20140396 and BK20140399), Opening Project of National Engineering Laboratory for Modern Silk (Grant No. KJS1511), Jiangsu Planned Projects for Postdoctoral Research Funds (Grant No. 1302112B), China Postdoctoral Science Foundation (Grant Nos. 2014M551656 and 2016T90495), and Nantong Science and Technology Planning Project (Grant No. GY12015013).

## References

- [1] Chan, C. K., *et al.*, Solution-Grown Silicon Nanowires for Lithium-Ion Battery Anodes, *ACS Nano*, 4 (2010), 3, pp. 1443-1450
- [2] Yoo, J. K., *et al.*, Scalable Fabrication of Silicon Nanotubes and their Application to Energy Storage, *Advanced Materials*, 24 (2012), 40, pp. 5452-5456
- [3] Lee, B. H., *et al.*, Charge Transport Characteristics of High Efficiency Dyesensitized Solar Cells Based on Electrospun TiO<sub>2</sub> Nanorod Photoelectrodes, *The Journal of Physical Chemistry C*, 113 (2009), 51, pp. 21453-21457
- [4] Liu, Y., *et al.*, Templated Synthesis of Nanostructured Materials, *Chemical Society Reviews*, 42 (2013), 7, pp. 2610-2653
- [5] Chen, R. X., *et al.*, Mini-Review on Bubbfil Spinning Process for Mass-Production of Nanofiber, *Materia*, 19 (2014), 4, pp. 325-343
- [6] He, J.-H., *et al.*, Control of Bubble Size and Bubble Number in Bubble Electrospinning, *Computers and Mathematics with Applications*, 64 (2012), 18, pp. 1033-1035
- [7] He, J.-H., *et al.*, Effect of Temperature on Surface Tension of a Bubble and Hierarchical Ruptured Bubbles for Nanofiber Fabrication, *Thermal Science*, 16 (2012), 1, pp. 325-328
- [8] Li, Z., *et al.*, Electrostatic Forces Induce Poly (Vinyl Alcohol) Protected Copper Nanoparticles to Form Copper/Poly (Vinyl Alcohol) Nanocables via Electrospinning, *Macromolecular Rapid Communications*, 27 (2006), 2, pp. 152-155
- [9] Tao, D., *et al.*, PA6 Nanofiber Chemical Copper Plating Research, *Journal of Synthetic Fiber Industry*, 31 (2009), 3, pp. 24-26
- [10] Bergshoef, M. M., *et al.*, Transparent Nanocomposites with Ultrathin, Electrospun Nylon-4, 6 Fiber Reinforcement, *Advanced Materials*, 11 (1999), 16, pp. 1362-1365

Paper submitted: December 2, 2015

Paper revised: February 1, 2016

Paper accepted: February 11, 2016